AGU PUBLICATIONS

Water Resources Research

TECHNICAL REPORTS: METHODS

10.1002/2016WR018954

Key Points:
- Contact spectroscopy excels at characterizing spatiotemporal variation in snowpack microstructure
- Proximity to tree canopy influences snowpack temperature gradient and snow grain growth
- Rates of snow metamorphism are significantly greater on south versus north sides of trees

Supporting Information:
- Supporting Information S1

Correspondence to:
N. P. Molotch,
noah.molotch@colorado.edu

Citation:
Molotch, N. P., D. M. Barnard, S. P. Burns, and T. H. Painter (2016), Measuring spatiotemporal variation in snow optical grain size under a subalpine forest canopy using contact spectroscopy, *Water Resour. Res.*, *52*, doi:10.1002/2016WR018954.

Received 20 MAR 2016
Accepted 10 SEP 2016
Accepted article online 16 SEP 2016

Measuring spatiotemporal variation in snow optical grain size under a subalpine forest canopy using contact spectroscopy

Noah P. Molotch[1,2,3], David M. Barnard[1], Sean P. Burns[2,4], and Thomas H. Painter[3]

[1]Institute of Arctic and Alpine Research, University of Colorado, Boulder, Colorado, USA, [2]Department of Geography, University of Colorado, Boulder, Colorado, USA, [3]Jet Propulsion Laboratory, California Institute of Technology, Pasadena, California, USA, [4]National Center for Atmospheric Research, Boulder, Colorado, USA

Abstract The distribution of forest cover exerts strong controls on the spatiotemporal distribution of snow accumulation and snowmelt. The physical processes that govern these controls are poorly understood given a lack of detailed measurements of snow states. In this study, we address one of many measurement gaps by using contact spectroscopy to measure snow optical grain size at high spatial resolution in trenches dug between tree boles in a subalpine forest. Trenches were collocated with continuous measurements of snow depth and vertical profiles of snow temperature and supplemented with manual measurements of snow temperature, geometric grain size, grain type, and density from trench walls. There was a distinct difference in snow optical grain size between winter and spring periods. In winter and early spring, when facetted snow crystal types were dominant, snow optical grain size was 6% larger in canopy gaps versus under canopy positions; a difference that was smaller than the measurement uncertainty. By midspring, the magnitude of snow optical grain size differences increased dramatically and patterns of snow optical grain size became highly directional with 34% larger snow grains in areas south versus north of trees. In winter, snow temperature gradients were up to 5–15°C m^{-1} greater under the canopy due to shallower snow accumulation. However, in canopy gaps, snow depths were greater in fall and early winter and therefore more significant kinetic growth metamorphism occurred relative to under canopy positions, resulting in larger snow grains in canopy gaps. Our findings illustrate the novelty of our method of measuring snow optical grain size, allowing for future studies to advance the understanding of how forest and meteorological conditions interact to impact snowpack evolution.

1. Introduction

The processes controlling the distribution of snow grain size are highly variable across the landscape. In forested regions, which represent 40% of snow-covered landscapes globally [*Klein et al.*, 1998; *Stueve et al.*, 2011], forest canopy structure exerts significant influence on snow depth, snow water equivalent (SWE), and snow microstructure [*Faria et al.*, 2000; *Molotch et al.*, 2009; *Musselman et al.*, 2008; *Veatch et al.*, 2009; *Varhola et al.*, 2010; *Lundquist et al.*, 2013].

At higher latitudes (e.g., 50–60°), subcanopy net radiation and snowmelt rates can be positively correlated with canopy density when the ratio of canopy height to canopy gap width exceeds 1. Canopy interception of snow often yields decreasing snow depth from crown-edge to tree trunks [*Faria et al.*, 2000], and therefore rates of snowpack metamorphism and grain size growth may increase with proximity to tree trunks. In midlatitude regions (30–40°), however, much less is known about these interactions as lower solar zenith angles often causes net radiation to decrease with increasing canopy density [*Molotch et al.*, 2011].

Understanding the effect of forest canopy on snow metamorphic rates is necessary to mathematically represent the physics of snow evolution under forest canopies. Such an understanding is a vital step to explicitly representing snow/vegetation interactions in distributed hydrologic and land surface models. In addition, detailed measurements of snowpack properties, such as snow grain size, are needed across gradients in forest structure to constrain snowpack energy and mass balance models [*Bartelt and Lehning*, 2002; *Brun et al.*, 1992; *Jordan*, 1991; *Lehning et al.*, 2002]. The controls on snow grain size variability are largely unstudied given the measurement constraints discussed above. However, controls on snow depth and snowmelt have been widely studied [e.g., *Broxton et al.*, 2014; *Faria et al.*, 2000; *Musselman et al.*, 2012a, 2012b] and thus first-order hypotheses regarding controls on snow grain size can be derived as kinetic growth metamorphism is largely controlled by variability in air temperature, snow depth, and resulting snow temperature gradients [*Giddings and LaChapelle*, 1962]. Vegetation influences snow depth by intercepting snow, attenuating incoming solar radiation, emitting thermal radiation to the snow surface, and decreasing wind speed which causes variability in turbulent fluxes between canopy gaps and under-canopy locations [*Lundquist et al*., 2013]. The combination of varying snow depth and energy fluxes associated with canopy structure results in variations in thermal gradients within the snowpack that strongly influence snowpack metamorphism [*Sturm*, 1992].

To date the influence of coniferous vegetation on snowpack microstructure has not been documented. As a result, linkages between vegetation-altered energy fluxes and spatial patterns of snow cover ablation have not been made. Hence, improved quantification of the influence of vegetation on snow metamorphism across vertical and horizontal gradients is needed. In this research, we use field spectroscopy coupled with contact illumination [*Painter et al*., 2007] to measure the vertical and horizontal stratigraphic distribution of snow optical grain size in snow trenches excavated surrounding coniferous vegetation. The application of contact spectroscopy illustrated herein builds upon previous works [e.g., *Painter et al*., 2007] by resolving both vertical and horizontal variability in snow optical grain size. This is an important distinction given that snow optical grain size can vary horizontally over relatively short (i.e., $<$10 m) length scales associated with vegetation structure [*Musselman et al*., 2008]. Using this snow optical grain size measurement technique, we quantified the spatiotemporal variation in snow optical grain size surrounding vegetation. The following two questions are addressed: (1) What is the variability in snow optical grain size at the stand scale? and (2) How does optical grain size variability change throughout the snow season?

The application of spectroscopy to measuring snow/vegetation interactions is a new methodology with the potential to advance understanding of the linkages between vegetation and snowpack microstructure beyond any previous attempts.

2. Methods

2.1. Study Area

This study was conducted at the Niwot Ridge Subalpine Forest AmeriFlux site (site: US-NR1) located 8 km east of the Continental Divide at an elevation of 3050 m (latitude 40.0329°N, longitude 105.5464°W). Tree density at the site is approximately 0.4 trees m^{-2}, tree heights are typically between 11 and 13 m, leaf area index is 3.8–4.2 m^2 m^{-2}, and canopy gap fraction is approximately 18%. Gaps studied ranged in dimension from 300 to 490 cm from tree bole to tree bole. Gaps were generally elliptical in shape. Trench locations were selected to maintain the north-south and east-west gap orientations required for the experiment design. All trenches were located in an area within 50 m of the North Canopy Tower (Figure S1) which is adjacent to the Niwot Ridge AmeriFlux Tower (http://fluxnet.ornl.gov/site/997). Snow depth and snow temperature sensors were positioned within 10 m of the North Canopy Tower and therefore the trenches were all within 50 m of all data used in this study; see *Burns et al*. [2014] for a site map of flux tower and snow temperature probes. A mixture of conifer species are present at the site including subalpine fir (*Abies lasiocarpa*), Engelmann spruce (*Picea engelmannii*), and lodgepole pine (*Pinus contorta*). Further description of the site can be found in *Turnipseed et al*. [2002].

2.2. Snow Grain Size Measurements Using Contact Spectroscopy

Measurements of all snow properties were collected during four intensive measurement periods in which spectroscopic measurements of snow grain size were made in trenches dug in cardinal directions between eight previously selected pairs of trees (Figure 1). The first measurement period (26 and 28 February 2006) was intended to study snow vegetation interactions in midwinter. The second measurement period (24 and 25 March 2006) focused on early spring snowpack. The third measurement period (19 and 20 April 2006) represented melt-transition snowpack conditions and the fourth measurement period (16 May 2006) represented the late-snowmelt period. Meteorological conditions during each sampling period are presented in Table S1.

Characterizing the influence of vegetation on snow metamorphism is challenging using standard procedures (i.e., a hand lens) because it is time-consuming and lacks repeatability. To reduce the field time

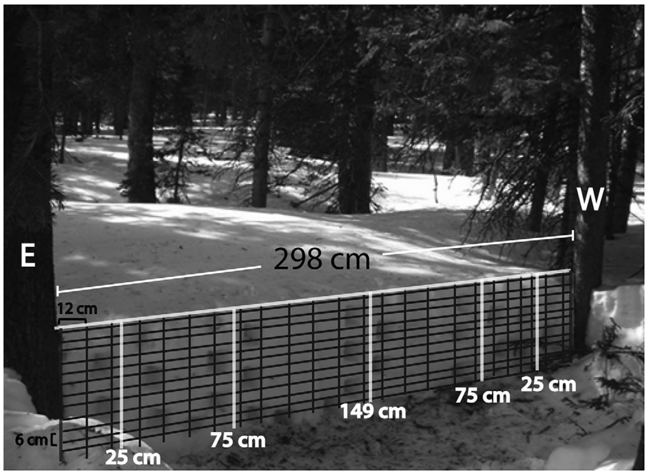

Figure 1. Photograph of representative snow trench between two trees used for snow sampling. Grain size measurements were made within each rectangle illustrated by the black mesh. Manual vertical profiles of snow temperature, snow density, snow grain size, and crystal type are denoted by the vertical white lines.

required to obtain measurements of snow optical grain size, we use an Analytical Spectral Devices FR field spectroradiometer (ASD-FR) coupled with an ASD high-intensity contact probe to directly observe optically equivalent grain radius horizontally and vertically using the method of *Painter et al*. [2007]. Note that hereafter where we use the term *snow grain size* interchangeably with the term *snow optical grain size*; an important distinction given recently published snow terminology guidelines [*Fierz et al*., 2009].

The ASD-FR samples reflectance, radiance, and irradiance in the wavelength range 350–2500 nm at 3–10 nm spectral resolution. We then analyze ASD-FR spectra for snow grain size by relating the measured depth of the ice absorption feature centered at 1020 nm to modeled reflectance of spherical ice particles [*Painter et al*., 2007; *Nolin and Dozier*, 2000]. This technique is not unique with respect to the spherical particle assumption [e.g., *Picard et al*., 2009; *Libois et al*., 2013] as previous works have related observed reflectance to modeled spectra in the short-wave infrared portion of the spectrum [*Gallet et al*., 2009; *Arnaud et al*., 2011]. Previous work has shown that the method of grain size retrieval has a root mean square error of 74 μm when using airborne data [*Painter et al*., 2003], with errors reduced (i.e., 10–50 μm) when using contact spectroscopy given that several sources of uncertainty are reduced when observing reflectance from the ground [*Painter et al*., 2007].

Spectral measurements were distributed across the snow trench face at 6 cm vertical spacing and 12 cm horizontal spacing (Figure 1); intervals were maintained using a gridded mesh staked to the snow pit face. Spectral measurements were made using an aluminum spacer 1 cm in length which prevented the contract probe from making contact with the snow pit face; this is required so that the heat of the light source does not increase snow grain size. Prior to collecting spectra 10 spectral measurements were made of a 99% reflectance reference standard. Ten reference spectra were also collected in between each vertical sampling column shown in Figure 1; this is required given that the spectrometer drifts over time. The groups of 10 reference spectra were averaged and were then interpolated in time to characterize spectrometer drift. Collected snow spectra were then normalized by the interpolated reference measurements; further details are provided in *Painter et al*. [2007].

Our approach is unique in that information will be obtained horizontally and vertically from tree bole to tree bole, whereas previous work has focused only on properties of the surface snow or paired vertical profiles [*Painter et al*., 2007]. This important step will extend existing hyperspectral approaches for snow to a two-dimensional (and by extension 3-D) domain. These two-dimensional, vertical arrays of snow grain size measurements were spline interpolated to generate continuous images of the distribution of snow grain size. This interpolation is necessary given that the spatial resolution of the contact probe measurement (i.e., approximately 2 cm) is significantly smaller than the aforementioned spacing of the measurements. The resultant images illuminate previously unexplored interactions between forests and snow. Average grain size values in under-canopy positions and canopy gaps are reported which represent the horizontal and vertical mean values in each position.

2.3. Continuous Snow Depth and Snow Temperature Observations

Continuous snow and soil temperature measurements were made at 10 cm vertical intervals using three TP101 thermistor temperature probes (Measurement Research Corporation, Harbor, WA, USA) at depths of −12 to 88 cm (under canopy), −12 to 188 cm (canopy gap), and −15 to 185 cm (canopy edge), where negative numbers represent distances below the snow-soil interface. The probes were inserted into the soil prior to snow accumulation and snow was allowed to naturally accumulate around the thermistor probes.

Vertical profiles of snow temperature gradients were calculated as the difference in temperature between two sensors, divided by the distance between sensors (10 cm). In the case of the lowest profile, the highest soil temperature probe was used. Snow temperature gradient for the lower 40 cm of the snowpack was then calculated as the average of the profiles at or below 40 cm.

The three probes were placed at distances of 20, 60, and 180 cm from an adjacent tree bole to measure under-canopy (20 cm location), canopy-edge/drip-line (60 cm), and canopy-gap (180 cm) locations. Continuous snow depth measurements were obtained using ultrasonic distance sensors (Judd Communications) positioned in under-canopy, canopy-edge, and canopy-gap locations; three sensors in each position for a total of nine sensors. More information and technical description of the temperature and snow depth measurements can be found in *Burns et al*. [2014] and *Molotch et al*. [2007, 2009], respectively.

2.4. Manual Profile Measurements

Along each trench, five vertical profiles of snow temperature, snow grain size, snow grain morphology, and snow density were observed manually. Given the time required for the spectral measurements, these profiles were sampled 3–4 h after initial snow trench excavation and therefore trench walls were shaved back about 30 cm to ensure sampling of undisturbed snow. Profiles were spaced horizontally at distances of 25 and 75 cm from each tree bole and a center profile (Figure 1), representing subcanopy, canopy edge, and canopy gap conditions, respectively. The center profile was positioned to be equidistant from the two tree boles at the center of the trench. The canopy-edge profile position (75 cm) was selected to ensure measurements were acquired under the canopy but near the canopy edge; crown radii were approximately 1 m on average.

Along each profile, snow density measurements were made using a 1 L stainless steel cutter at 10 cm vertical increments from the snow-atmosphere interface to the ground-snow interface. Snow temperature measurements were made at 10 cm intervals from the ground-snow interface to the snow-atmosphere interface using a dial stem thermometer which had been calibrated to 0°C in an ice bath. Snow grain size and morphology measurements were made using a hand-held magnifier with 25-fold magnification and graduated ruler with a precision of 0.1 mm. Observations were made for discrete snow layers identified via hardness tests using a thin stainless steel putty knife.

3. Results

3.1. Snow Grain Size From Contact Spectroscopy

The vertical and horizontal variability in snow grain size was distinctly different during premelt (February and March) versus snowmelt periods (April and May) (Figures 2a–2h and 3a–3h). On 26 February, grain size images reveal a vertical grain size gradient in which snow grain size increased from the snow-atmosphere interface to the snow-ground interface (Figures 2a and 2b). Corresponding hand lens observations indicated a facetted crystal structure across the sampling domain (Figure S2). In addition, surface layer snow grain size was 2–3X smaller than in the basal layer during the February and March trenches. The vertical grain size gradients were variable across the images from tree bole to tree bole with canopy gap positions in the February and March images exhibiting 6% larger grain size values versus under-canopy positions ($p = 0.01$); note these differences do not exceed the measurement RMSE of 74 μm.

Grain size patterns on 24 and 25 March were typical of a continental snowpack with larger facetted snow grains at depth and smaller rounded snow grains closer to the surface (Figures 2c and 2d). Qualitatively, the influence of vegetation on snow grain size in the depth hoar layer (i.e., below the black line in Figures 2c and 2d) was different than in the surface layer (i.e., above the black line in Figures 2c and 2d). Grain size was 6% greater on the south versus north sides of trees, with the northern versus southern halves of the trench having mean grain radii of 177 μm versus 169 μm, respectively (Figure 3d and Table S2). Conversely, grain sizes for the depth hoar layer did not vary directionally with slightly larger snow grains (3–7% larger) in the center of the clearing versus under the canopy and generally greater spatial variability than surface layers. It is important to note that validation of the spectral snow grain size measurement technique has not been conducted for facetted crystal structures such as depth hoar. Hence, the small grain size differences noted here are likely not significant in the context of measurement uncertainty.

With the progression of spring, the snow grain size patterns increasingly reflected directionality in the north-south direction, with increased grain size in areas with greater solar irradiance (i.e., areas to the south

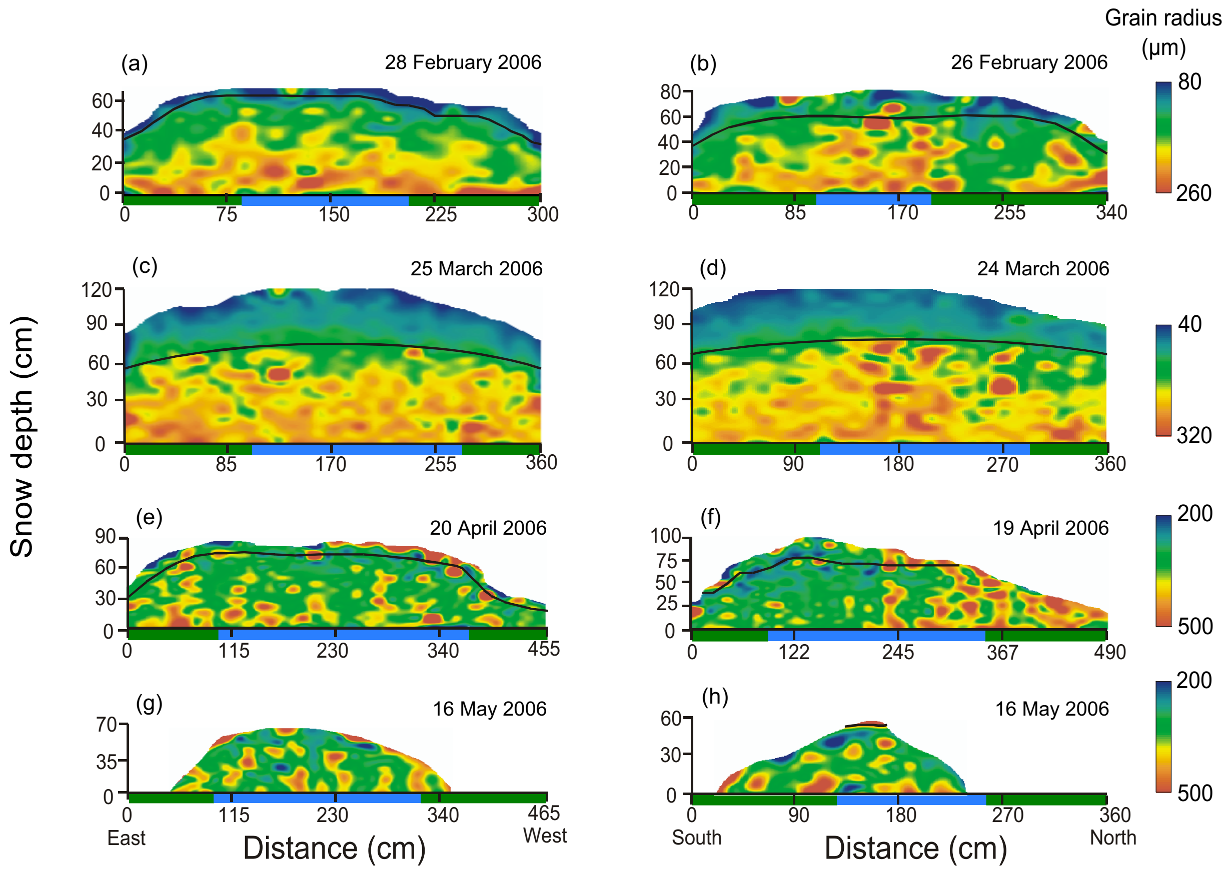

Figure 2. Distribution of snow grain size measured in snow trenches excavated between coniferous trees. Trenches were oriented in (a, c, e, g) east-west and (b, d, f, h) north-south directions. Black line indicates interface between facetted and rounded snow grains as determined using a hand lens. Minimum and maximum *x* axis values correspond to tree bole locations. Green bars under the *x* axis represent portions of the transect under the tree canopy whereas the blue bars represent portions exposed to open sky.

of trees). For example, during the 19 April measurements, areas south of the tree bole had a mean grain radius 34% greater than areas north of trees (i.e., 339 versus 253 μm, respectively; Figures 2f and 3f and Table S2). These patterns suggest enhanced solar irradiance increased surface melt and grain growth via wet metamorphism; manual hand lens observations on 19 April support this hypothesis as liquid water was observed on the south side of trees but not on the north side. This radiation-driven spatial pattern was not observed along the east-west trench (Figures 2e and 3e) as solar irradiance is more uniform in the east-west versus north-south directions.

The horizontal patterns in snow metamorphism and grain size observed in March and April led to similar patterns in snow ablation observed on 16 May. In this regard, preferential ablation occurred in exposed areas to the south side of trees as a result of the enhanced surface melt (Figure 2h). The ablation pattern on the east and west sides of the trees were relatively similar (Figure 2g), further suggesting that interactions of solar and thermal radiation and canopy structure play an important role in the distribution of snow grain size, metamorphism and snowmelt.

3.2. Snow Depth, Snow Temperature, and Snow Metamorphism

Continuous observations of snow depth and snow temperature offer insights into the snow grain size patterns observed in Figures 2a–2h as snow depth and snow temperature gradients influence equilibrium and kinetic metamorphism. These measurements illustrate that the controls on snow grain size shift from being dominated by snow temperature gradients in fall and winter to being dominated by interactions between solar radiation and canopy structure in spring. The details of these observations are described below.

Under-canopy position snow depth was, on average, measured to be 55% of the snow depth measured at the canopy-gap (Figure 4a). This has implications for the compressive forces governing snow grain growth

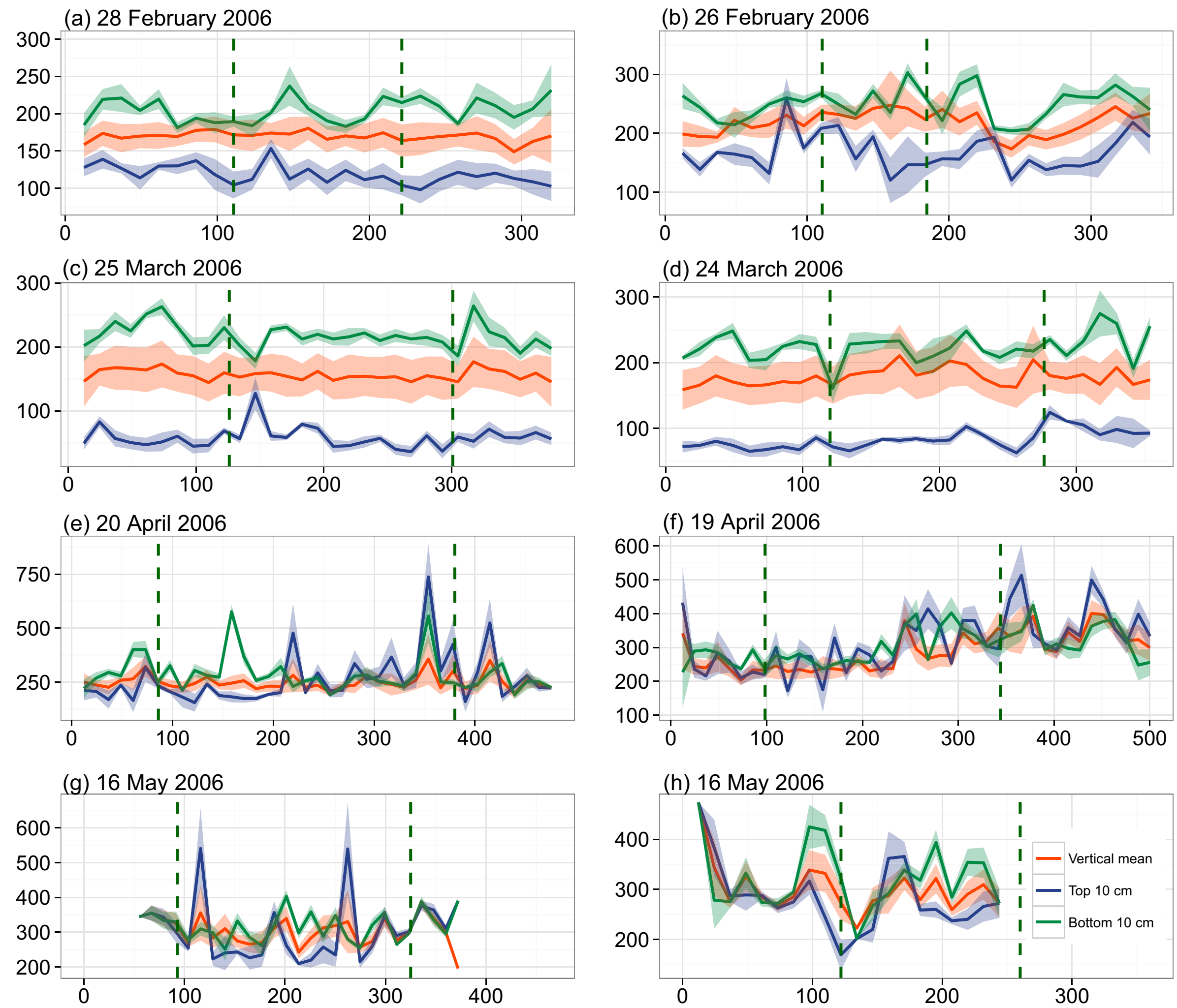

Figure 3. Mean values of snow grain radius for the top and bottom 10 cm of the snowpack and for the entire snow depth (i.e., vertical mean). Shading around each line represents one standard deviation on either side of the mean. Vertical dashed lines represent canopy edge locations for each sampling period with canopy gaps located between the dashed lines.

via equilibrium metamorphism and for the temperature gradients that govern kinetic growth metamorphism [*McClung and Shaerer*, 1993]. The data shown in Figure 4b indicate that strong temperature gradients commonly occur in fall and were greater in under-canopy positions versus canopy gaps (Figures 4b and 4c and Table S2). During the early winter period (i.e., DOWY 84–152; 22 December to 26 February), additional snowfall resulted in decreased snow temperature gradients which would decrease kinetic metamorphism grain growth rates. However, because snow accumulation was significantly lower in under canopy positions (Figure 4a), snow temperature gradients remained relatively high under the canopy versus canopy gaps. Manually observed temperature gradients were 1.7°C m^{-1} greater under the canopy than in canopy gaps on 26 and 28 February (Figure S3), supporting the observations from the automated sensors (Figure 4b). Differences in temperature gradient among the three thermistor locations varied by as much as 5–15°C m^{-1}, with the largest variation occurring in early season (i.e., before DOWY 82; Figure 4c). Hence, significant variability in kinetic snow metamorphism likely occurred given that temperature gradients drive vapor gradients within the snowpack. While this is a large difference in snow temperature gradient, the canopy positions exhibited significant differences in snow depth and therefore this level of variability in snow temperature gradient is not entirely surprising.

The spring transitional period (i.e., DOWY 152–180) showed different snow temperature gradients in the different canopy positions, with under-canopy positions maintaining a stronger snow temperature gradient for much of this period. For example, on 24 March, manually observed temperature gradients under the

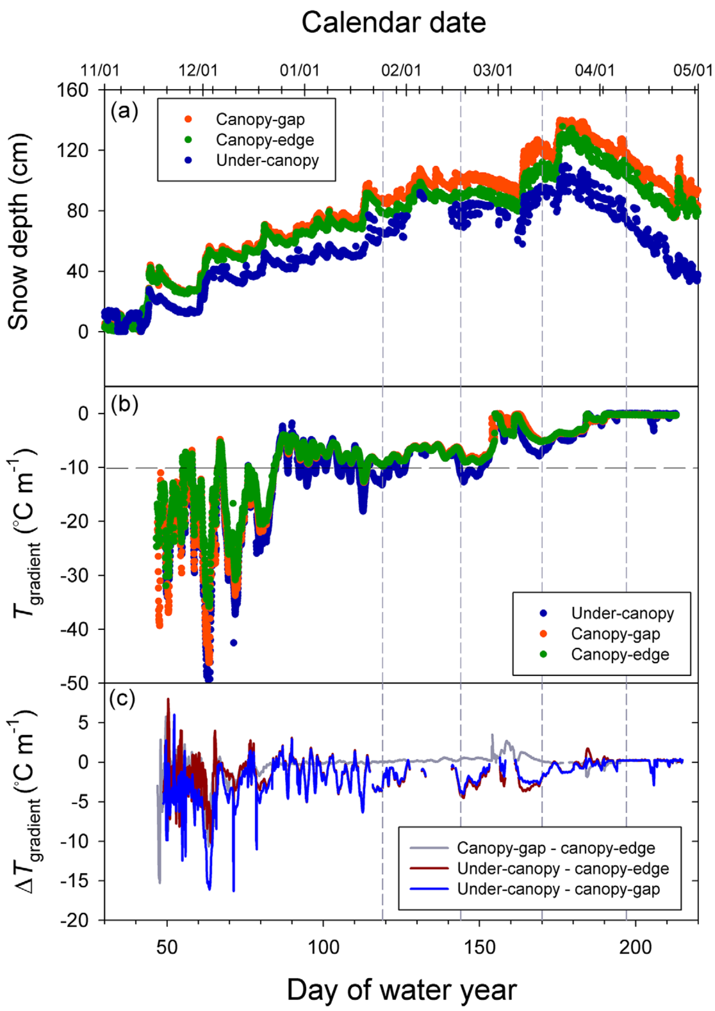

Figure 4. (a) Snow depth and (b) snow temperature gradient ($T_{gradient}$) in the snowpack at under-canopy, canopy-gap, and canopy-edge locations; horizontal dashed line in Figure 4b demarks the threshold for kinetic growth metamorphism. Snow temperature gradients were calculated at 30 min time steps for the lower 40 cm of the snowpack if snow depth was greater than 40 cm; otherwise, the temperature gradient represents the entire snow profile. This minimizes the influence of short-term fluctuations near the snow surface. Figure 4c shows temperature gradient differences ($\Delta T_{gradient}$) among the three canopy positions in which the second position listed in the legend is subtracted from the first (e.g., under-canopy − canopy-gap). Vertical dashed lines indicate the timing of the spectral snow grain size measurements.

canopy were 1.1°C m^{-1} greater in magnitude than those measured in canopy gaps (i.e., more negative). On 19 April, the differences in manually observed temperature gradients increased to 3°C m^{-1} and the snowpack had become isothermal in exposed areas such as canopy gaps and areas to the south of trees. Hence, the higher snow temperatures in exposed areas contributed to relatively greater rates of equilibrium and wet metamorphism. These observations and interpretations are consistent with the April snow grain size images (Figures 2e and 2f) whereby areas with greater solar irradiance (i.e., canopy gaps and under-canopy positions to the south trees) exhibited a snow grain stratigraphy consistent with spring transitional snow (i.e., wet, large grains at the surface) whereas under-canopy shaded areas exhibited snow stratigraphy patterns consistent with a winter snowpack (i.e., dry, large, faceted grains at depth).

3.3. Snow Density

Consistent with a transition from a winter to spring snowpack, mean snow density (average of north-south and east-west transects) increased throughout the season from 251 kg m^{-3} in February to 343 kg m^{-3} in May. Interestingly, vertical and horizontal spatial variation in snow density was lowest in early winter (i.e., February) and late spring (i.e., May) with a mean coefficient of variation (CV) from all four cardinal directions of 7.2 and 8.3%, respectively. Conversely, snow density during early and midspring (i.e., March and April) was more variable with CV values of 18.8 and 12.7%, respectively. The timing of snow density transitions in spring was heavily influenced by canopy structure with dry, lower density snow layers under the canopy in the shade of trees and wet, higher snow density layers in areas with greater solar irradiance.

4. Discussion

The time series of snow grain size measurements shown in Figure 2 have utility for constraining snowpack energy and mass balance models which have grain size as a state variable [*Bartelt and Lehning*, 2002; *Brun et al*., 1992; *Jordan*, 1991; *Lehning et al*., 2002]. While measurements of optically equivalent snow grain size, reported here, are not analogous to the geometric grain size represented within these models, recent advances in model development have afforded explicit representation of optical snow grain size

[*Carmagnola et al*., 2014]. In addition previous work has shown that statistically significant relationships between optically equivalent and geometric grain size exist ($r^2 = 0.72$; $p < 0.01$) [*Perrot et al*., 2014]. However, these relationships may not be consistent for snow crystals with significant variability in morphology such as mixtures of facetted and rounded crystal types [*Langlois et al*., 2010].

Variability in snow grain size measurements must be viewed in the context of uncertainty in the spectral measurements. Given the RMSE of the grain size measurements of 74 μm [*Painter et al*., 2003], the subtle differences in grain size with canopy position in February and March are not significant relative to the magnitude of sampling error. Importantly, however, the horizontal differences in grain size observed along the north-south trench far exceeded the measurement error and therefore the increased directionality in grain size during the spring transition is a statistically robust result.

In addition to constraining model representations of snow grain size, the snow grain size data have implications for spatially distributed snowmelt models. These models often rely on depletion curves which relate snow cover extent to snow water equivalent or cumulative snowmelt [e.g., *Durand et al*., 2008; *Molotch*, 2009]. When based on empirical observations from satellite, these methods effectively assume that snow cover fraction detected in viewable, canopy-free areas, is equivalent to snow cover fraction in undetectable, under-canopy locations. Given that many of these models include snow grain size as a state variable, the grain size measurements presented here could be used to evaluate model representations of grain size in canopy-free and under-canopy locations. These evaluations have important implications for the development of parameterizations of model forcings governing snow cover ablation in canopy gaps versus under-canopy locations (e.g., canopy attenuation of solar radiation and wind speed). In this regard, *Lundquist et al*. [2013] found that the difference between midwinter snowmelt rates under the canopy, versus canopy gaps, largely controls the difference in snow disappearance timing between gaps and under canopy positions. Our work provides mechanistic insights on these processes in that the greater snow temperature gradients observed under the canopy suggest that variability in snow metamorphism, and by extension snowmelt, associated with canopy structure is affected by both energy inputs (i.e., net radiation) and variability in snow depth.

Conceptual models presented in *Molotch et al*. [2011] suggest that time periods/locations with greater (lower) solar zenith angles and lower (greater) solar irradiance will have greater (lower) net radiation under the canopy versus in gaps. Observations of snow grain size in April, when solar zenith angles were relatively low, reflect this behavior as larger rounded surface snow grains were observed in gaps and to the south of trees (Figure 2f), indicating greater surface energy inputs (i.e., net radiation) in these areas.

The increased depth hoar development in canopy gaps may have occurred because the snow was deeper in these locations at a time when kinetic metamorphism was dominating. In this regard, previous works have shown that differences in snow depth between gaps and under the canopy are greater when the snowpack is thinner [*López-Moreno and Latron*, 2008; *Revuelto et al*., 2015]. The increased development of depth hoar in canopy gaps is somewhat counter-intuitive because, mathematically, temperature gradients must decrease when snow depth increases. However, the observed temperature gradients in fall (Figure 4b) far exceeded the threshold 10°C m^{-1} temperature gradient needed for kinetic metamorphism [*McClung and Schaerer*, 1993]. Hence, more significant depth hoar development in canopy gaps may have occurred simply because the snow depth was greater in these areas at a time period when kinetic metamorphism was dominant.

Varhola et al. [2013] argue that the myriad sources of variability in snow-forest interactions make it difficult to identify general behavior and therefore new experimental designs that measure as many sources of variability as possible are needed. The method presented here partially addresses this need by providing detailed observations that link variability in snow accumulation and snowmelt by resolving the intermediate processes governing the distribution of snow microstructure.

Notwithstanding, the experiment conducted here could be improved in a number of ways. First, observed snow crystals were exposed to the atmosphere within the snow trench for a relatively long period of time (e.g., 2+ h) as the sampling is time-consuming. Second, the sampling method used is destructive in that a trench is dug in the snow and hence the exact same location cannot be revisited at a later date. Both of these issues could be partly addressed by employing a probe-mounted spectral retrieval system [e.g., *Berisford et al*., 2013]. Third, light contamination from the sun may have impacted the grain size retrievals. This issue could be addressed by sampling at night or by making measurements under a large opaque blanket. Fourth, the addition of ancillary measurements focused on snow-forest interactions should be considered; e.g., iButtons (Maxim Integrated Inc.), time-laps cameras, and fiber-optic cables have shown great promise in observing spatial variation in snow cover persistence at the stand scale [*Dickerson-Lange et al*., 2015]. Finally, while our stand characteristics were fairly uniform from trench to trench (by design), the methods illustrated here could be extended to different canopy structures to further explore the influence of canopy structure on snow metamorphism and snow ablation. The complexity of terrain and vegetation-induced variability in snow properties highlights the need for improved methods of measuring horizontal variability in snowpack properties such as those presented herein.

5. Conclusion

Using a unique snow grain size measurement approach within trenches dug from tree bole to tree bole, we revealed a distinct difference in snow grain size between winter and spring periods and between under-canopy canopy gap positions. In winter (i.e., February), when facetted snow crystal types were dominant, snow grain size was 6% larger in canopy gaps versus under canopy positions; a pattern that did not vary in the four cardinal directions around trees. During the snowmelt period (i.e., April), however, patterns of snow grain size became highly directional with 34% larger snow grains in areas south versus north of trees. In winter, snow temperature gradients were greater in under-canopy versus canopy gap positions. In spring, snow temperature gradients remained mostly negative in under-canopy shaded positions, whereas snow in canopy gaps and along the south sides of trees was isothermal, suggesting that variation in solar irradiance influenced grain size distribution. These spatial patterns in snow grain size were similar to patterns of snowmelt as snow ablation occurred earlier on the south sides of trees. Our findings illustrate the utility of this method of measuring snow grain size, allowing for future studies to advance the understanding of how forest and meteorological conditions interact to impact snowpack evolution.

Acknowledgments
This work was supported by the U.S. National Aeronautics and Space Administration under grant NNXIIAK35A, by the U.S. National Science Foundation (NSF) under grant EAR 1141764, and by the U.S. Department of Agriculture under grant 2012-67003-19802. Additional support was provided by the NSF Niwot Ridge Long Term Ecological Research program and by the Department of Energy Ameriflux program. Part of this work was conducted at the Jet Propulsion Laboratory, California Institute of Technology under contract from NASA. Snow grain size data sets can be downloaded from ftp://snowserver.colorado.edu/pub/NWT_snow_grain_size_trenches2006/grainSize.zip. All meteorological data can be obtained from http://fluxnet.ornl.gov/site/997.

References

Arnaud, L., G. Picard, N. Champollion, F. Domine, J.-C. Gallet, E. Lefebvre, M. Fily, and J.-M. Barnola (2011), Measurement of vertical profiles of snow specific surface area with a 1 cm resolution using infrared reflectance: Instrument description and validation, *J. Glaciol.*, *57*, 17–29, doi:10.3189/002214311795306664.

Bartelt, P., and M. Lehning (2002), A physical SNOWPACK model for the Swiss avalanche warning: Part I: Numerical model, *Cold Reg. Sci. Technol.*, *35*, 123–145.

Berisford, D. F., N. P. Molotch, M. T. Durand, and T. H. Painter (2013), Portable spectral profiler probe for rapid snow grain size stratigraphy, *Cold Reg. Sci. Technol.*, *85*, 183–190.

Broxton, P. D., A. A. Harpold, J. A. Biederman, P. A. Troch, N. P. Molotch, and P. D. Brooks (2014), Quantifying the effects of vegetation structure on snow accumulation and ablation in mixed-conifer forests, *Ecohydrology*, *8*, 1073–1094.

Brun, E., P. David, M. Sudul, and G. Brunot (1992), A numerical model to simulate snow-cover stratigraphy for operational avalanche forecasting, *J. Glaciol.*, *38*, 13–22.

Burns, S. P., N. P. Molotch, M. W. Williams, J. F. Knowles, B. Seok, R. K. Monson, A. A. Turnipseed, and P. D. Blanken (2014), Snow temperature changes within a seasonal snowpack and their relationship to turbulent fluxes of sensible and latent heat, *J. Hydrometeorol.*, *15*, 117–142.

Carmagnola, C. M., S. Morin, M. Lafaysse, F. Domine, B. Lesaffre, Y. Lejeune, G. Picard, and L. Arnaud (2014), Implementation and evaluation of prognostic representations of the optical diameter of snow in the detailed snowpack model SURFEX/ISBA-Crocus, *Cryosphere*, *8*, 1–20, doi:10.5194/tc-8-1-2014.

Dickerson-Lange, S. E., J. A. Lutz, K. A. Martin, M. S. Raleigh, R. Gersonde, and J. D. Lundquist (2015), Evaluating observational methods to quantify snow duration under diverse forest canopies, *Water Resour. Res.*, *51*, 1203–1224.

Durand, M., N. P. Molotch, and S. A. Margulis (2008), A Bayesian approach to snow water equivalent reconstruction, *J. Geophys. Res.*, *113*, D20117, doi:10.1029/2008JD009894.

Faria, D. A., J. W. Pomeroy, and R. L. H. Essery (2000), Effect of covariance between ablation and snow water equivalent on depletion of snow-covered area in a forest, *Hydrol. Processes*, *14*, 2683–2695.

Fierz, C., R. L. Armstrong, Y. Durand, P. Etchevers, E. M. Greene, D. M. McClung, K. Nishimura, P. K. Satyawali, and S. A. Sokratov (2009), The International Classification for Seasonal Snow on the Ground, in *Paris IHP-VII Technical Documents in Hydrology*, vol. 83, IACS Contrib. 1, 90 pp., UNESCO-IHP, Paris.

Gallet, J.-C., F. Domine, C. S. Zender, and G. Picard (2009), Measurement of the specific surface area of snow using infrared reflectance in an integrating sphere at 1310 and 1550 nm, *Cryosphere*, *3*, 167–182, doi:10.5194/tc-3-167-2009.

Giddings, J. C., and E. LaChapelle (1962), The formation rates of depth hoar, *J. Geophys. Res.*, *67*, 2377–2383.

Jordan, R. (1991), A one-dimensional temperature model for a snow cover: Technical documentation for SNTHERM, *DTIC Doc. 89*, Cold Reg. Res. and Eng. Lab. (U.S.), Eng. Res. and Dev. Cent. (U.S.).

Klein, A. G., D. K. Hall, and G. A. Riggs (1998), Improving snow cover mapping in forests through the use of a canopy reflectance model, *Hydrol. Processes*, *12*, 1723–1744.

Langlois, A., A. Royer, B. Montpetit, G. Picard, L. Brucker, L. Arnaud, K. Goïta, and M. Fily (2010), On the relationship between snow grain morphology and in-situ near infrared calibrated reflectance photographs, *Cold Reg. Sci. Technol.*, *61*, 34–42.

Lehning, M., P. Bartelt, B. Brown, C. Fierz, and P. Satyawali (2002), A physical SNOWPACK model for the Swiss avalanche warning: Part II. Snow microstructure, *Cold Reg. Sci. Technol.*, *35*, 147–167.

Libois, Q., G. Picard, J. France, L. Arnaud, M. Dumont, C. M. Carmagnola, and M. King (2013), Influence of grain shape on light penetration in snow, *Cryosphere*, *7*, 1803–1818, doi:10.5194/tc-7-1803-2013.

Lopez-Moreno, J. I., and J. Latron (2008), Influence of canopy density on snow distribution in a temperate mountain range, *Hydrol. Processes*, *22*, 117–126.

Lundquist, J. D., S. E. Dickerson-Lange, J. A. Lutz, and N. C. Cristea (2013), Lower forest density enhances snow retention in regions with warmer winters: A global framework developed from plot-scale observations and modeling, *Water Resour. Res.*, *49*, 6356–6370.

McClung, D. M., and P. Schaerer (1993), *The Avalanche Handbook*, 271 pp., The Mt., Seattle, Wash.

Molotch, N. P. (2009), Reconstructing snow water equivalent in the Rio Grande headwaters using remotely sensed snow cover data and a spatially distributed snowmelt model, *Hydrol. Processes*, *23*, 1076–1089.

Molotch, N. P., P. D. Blanken, M. W. Williams, A. A. Turnipseed, R. K. Monson, and S. A. Marguilis (2007), Estimating subliation of intercepted and sub-canopy snow using eddy covariance systems, *Hydrol. Processes*, *21*, 1567–1575.

Molotch, N. P., P. D. Brooks, S. P. Burns, M. Litvak, R. K. Monson, J. R. McConnell, and K. Musselman (2009), Ecohydrological controls on snowmelt partitioning in mixed-conifer sub-alpine forests, *Ecohydrology*, *2*, 129–142.

Molotch, N. P., P. D. Blanken, and T. E. Link (2011), Snow: Hydrological and ecological feedbacks in forests, in *Forest Hydrology and Biogeochemistry*, pp. 541–555, Springer.

Musselman, K. N., N. P. Molotch, and P. D. Brooks (2008), Effects of vegetation on snow accumulation and ablation in a mid-latitude subalpine forest, *Hydrol. Processes*, *22*, 2767–2776. doi:10.1002/hyp.7050.

Musselman, K. N., N. P. Molotch, S. A. Margulis, M. Lehning, and D. Gustafson (2012a), Improved snowmelt simulations with a canopy model forced with photo-derived direct beam canopy transmissivity, *Water Resour. Res.*, *48*, W10509, doi:10.1029/2012WR012285.

Musselman, K. N., N. P. Molotch, S. A. Margulis, P. B. Kirchner, and R. C. Bales (2012b), Influence of canopy structure and direct beam solar irradiance on snowmelt rates in a mixed conifer forest, *Agric. Forest Meteorol.*, *161*, 46–56, doi:10.1016/j.agrformet.2012.03.011.

Nolin, A. W., and J. Dozier (2000), A hyperspectral method for remotely sensing the grain size of snow, *Remote Sens. Environ.*, *74*, 207–216.

Painter, T. H., J. Dozier, D. A. Roberts, R. E. Davis, and R. O. Green (2003), Retrieval of subpixel snow-covered area and grain size from imaging spectrometer data, *Remote Sen. Environ.*, *85*, 64–77, doi:10.1016/S0034-4257(02)00187-6.

Painter, T. H., N. P. Molotch, M. Cassidy, M. Flanner, and K. Steffen (2007), Contact spectroscopy for determination of stratigraphy of snow optical grain size, *J. Glaciol.*, *53*, 121–127.

Perrot, D., N. P. Molotch, K. N. Musselman, and E. T. Pugh (2014), Modelling the effects of the mountain pine beetle on snowmelt in a subalpine forest, *Ecohydrology*, *7*, 226–241.

Picard, G., L. Arnaud, F. Domine, and M. Fily (2009), Determining snow specific surface area from near-infrared reflectance measurements: Numerical study of the influence of grain shape, *Cold Reg. Sci. Technol.*, *56*, 10–17, doi:10.1016/j.coldregions.2008.10.001.

Revuelto, J., J. I. Lopez-Moreno, C. Azorin-Molina, and S. M. Vicente-Serrano (2015), Canopy influence on snow depth distribution in a pine stand determined from terrestrial laser data, *Water Resour. Res.*, *51*, 3476–3489.

Stueve, K. M., I. W. Housman, P. L. Zimmerman, M. D. Nelson, J. B. Webb, C. H. Perry, R. A. Chastain, D. D. Gormanson, C. Huang, and S. P. Healey (2011), Snow-covered Landsat time series stacks improve automated disturbance mapping accuracy in forested landscapes, *Remote Sens. Environ.*, *115*, 3203–3219.

Sturm, M. (1992), Snow distribution and heat flow in the taiga, *Arct. Alp. Res.*, *24*, 145–152.

Turnipseed, A. A., P. D. Blanken, D. E. Anderson, and R. K. Monson (2002), Energy budget above a high-elevation subalpine forest in complex topography, *Agric. Forest Meteorol.*, *110*(3), 177–201.

Varhola, A., N. C. Coops, M. Weiler, and R. D. Moore (2010), Forest canopy effects on snow accumulation and ablation: An integrative review of empirical results, *J. Hydrol.*, *392*, 219–233.

Varhola, A., and N. C. Coops (2013), Estimation of watershed-level distributed forest structure metrics relevant to hydrologic modeling using LiDAR and Landsat, *J. Hydrol.*, *487*, 70–86, doi:10.1016/j.jhydrol.2013.02.032.

Veatch, W., P. D. Brooks, J. R. Gustafson, and N. P. Molotch (2009), Quantifying the effects of forest canopy cover on net snow accumulation at a continental, mid-latitude site, *Ecohydrology*, *2*, 115–128.